Available online at www.sciencedirect.com
ScienceDirect
International Journal of Pharmaceutics 343 (2007) 59–68
INTERNATIONAL JOURNAL OF PHARMACEUTICS
www.elsevier.com/locate/ijpharm

The molecular conformation of Ibuprofen, $C_{13}H_{18}O_2$, through X-ray diffuse scattering

D.J. Goossens *, A.P. Heerdegen, T.R. Welberry, A.G. Beasley

Research School of Chemistry, The Australian National University, Canberra 0200, Australia

Received 11 September 2006; accepted 20 April 2007
Available online 3 May 2007

Abstract

A study of the three-dimensional distribution of the X-ray diffuse scattering from the pharmaceutical Ibuprofen (2-(4-isobutylphenyl)propionic acid, $C_{13}H_{18}O_2$) has been undertaken.

The most important aspects of the molecular flexibility have been isolated, as have key correlations between variables within a single molecule. Hence, aspects of the conformational space of the molecule *within* a crystalline environment have been outlined. For example the correlations between torsional twists on different bonds in the molecule (corresponding to the torsional angles on atoms C3, O1 and C11) have been established. Even though the atoms are on opposite sides of the phenyl group, there is a strong negative correlation between the torsional angle on C3 and that on C11. This shows that the ability to predict the conformation a fragment of a molecule will adopt based on the conformations of the fragment found in other molecules may be limited, as aspects of molecular geometry far from the fragment itself will have impact on its conformation.

Between molecules, the positional coordinate components which coincide with the direction of propagation of strong intermolecular contacts, particularly the –COOH–HOOC– dimerising interactions, are positively correlated. On the other hand, motions perpendicular to such directions, and rotations about the torsional angles, do not propagate strongly from molecule to molecule.

Keywords: Diffuse scattering; Molecular conformation; Ibuprofen

1. Introduction

Morphology and molecular conformation in pharmaceuticals are critical parameters, as they influence dissolution, storability and other medically and economically important properties. The relationships between molecular flexibility, conformation and crystal morphology have been explored using many techniques. For Ibuprofen alone authors have used data mining (Shankland et al., 1998) and X-ray and neutron single-crystal structure determinations (Shankland et al., 1996; Winn and Doherty, 1998) to explore these relationships, as well as various experimental studies of crystal growth morphology (Cano et al., 2001; Labhasetwar and Deshmukh, 1993; Perlovich et al., 2004).

In order to increase understanding of the relationship between molecular flexibility and molecular conformations *within* a crystalline environment, the diffuse scattering from racemic Ibuprofen has been studied. The diffuse scattering is descriptive of departures from the average structure, whether static or thermally activated. The forms these departures take depends on the flexibility of the molecule in the crystalline environment and how it interacts with its neighbours (Welberry, 2004). A molecule's motions affect the conformation and position of nearby molecules, causing a cooperative short-range ordering which cannot be seen using Bragg scattering (as used in conventional crystallography), and is not a property of a single molecule.

The crystal structure of racemic Ibuprofen (2-(4-isobutylphenyl)propionic acid, $C_{13}H_{18}O_2$) is monoclinic with $Z = 4$, spacegroup $P2_1/c$ and $a = 14.667$ Å, $b = 7.886$ Å, $c = 10.730$ Å and $\beta = 99.362^\circ$ (McConnell, 1974) at room temperature (see Fig. 1). It has been redetermined using neutron diffraction with similar results (allowing that the neutron work was performed at 100 K) (Shankland et al., 1997). A conformational analysis of Ibuprofen through database searching mapped out some aspect of 'the preferred conformational space' of the molecule (Shankland et al., 1998). Diffuse scattering analysis

* Corresponding author. Tel.: +61 2 6125 3536; fax: +61 2 6125 0750.
E-mail address: goossens@rsc.anu.edu.au (D.J. Goossens).

0378-5173/$ – see front matter © 2007 Elsevier B.V. All rights reserved.
doi:10.1016/j.ijpharm.2007.04.023

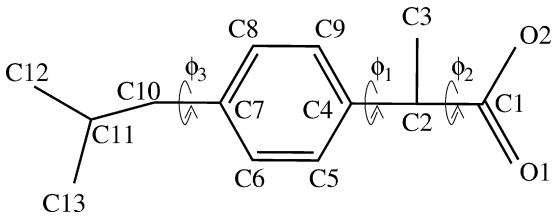

Fig. 1. Schematic diagram of the Ibuprofen molecule. H atoms omitted. Allowed torsional rotations noted as ϕ_1 to ϕ_3.

offers an alternative route to a similar result, one that depends not on the previously determined likely average conformations of molecular fragments but rather on the structured diffuse scattering which occurs between the Bragg peaks and results from the interactions between the molecules in a crystal. The aim is to construct a real-space model of the crystal whose diffuse scattering matches the observed. The model can then be analysed to explore the conformations of Ibuprofen molecules. A good fit gives confidence that these conformations are representative of those found in the real crystal.

2. Experimental

Single crystals of racemic Ibuprofen of sizes up to approximately 0.5 mm × 0.5 mm × 0.5 mm were grown by slow cooling of a saturated solution of Ibuprofen in acetonitrile. The solution was sealed into an air-tight tube, suspended in a computer-controlled waterbath and cooled from 38 °C to 30 °C over 5 days.

A smaller crystal grown in the same manner was used in a conventional single-crystal study to obtain a set of room temperature anisotropic atomic displacement parameters (ADPs), which were not available in the published structures (McConnell, 1974; Shankland et al., 1997). This was done because the short-range order model derived from the diffuse scattering must satisfy the average structure. In other words, averaging across the model crystal should recover the single-body average structure as given by Bragg peak studies. Hence good quality single-crystal data is a useful test of a short-range order model *and* a useful guide in developing that model in the first place.

Diffuse scattering data were collected at room temperature on the 1-ID-C beam line at the Advanced Photon Source. A 3D volume of data was collected and for analysis individual reciprocal space sections were extracted using the program XCAVATE (Estermann and Steurer, 1998; Scheidegger et al., 2000; Weber et al., 2001; Welberry et al., 2005). Appropriate symmetry was applied to each section to improve counting statistics.

The data were collected using an on-line mar345 image plate detector/reader system with a pixel resolution of 0.15 mm and 300 mm diameter, yielding 2000 pixel frames. The sample-to-detector distance was refined against a standard and found to be 297.6(1) mm. The photon energy was 40 keV, giving a wavelength of $\lambda = 0.30997(1)$ Å. Five hundred and twelve exposures were collected per sample, with the crystal rotated through 0.36° between exposures, giving a total of 184° angular coverage—enough to allow reconstruction of most of reciprocal space out to 9.6 Å^{-1} ($\sin(\theta)/\lambda = 0.764$ Å^{-1}). Fig. 2

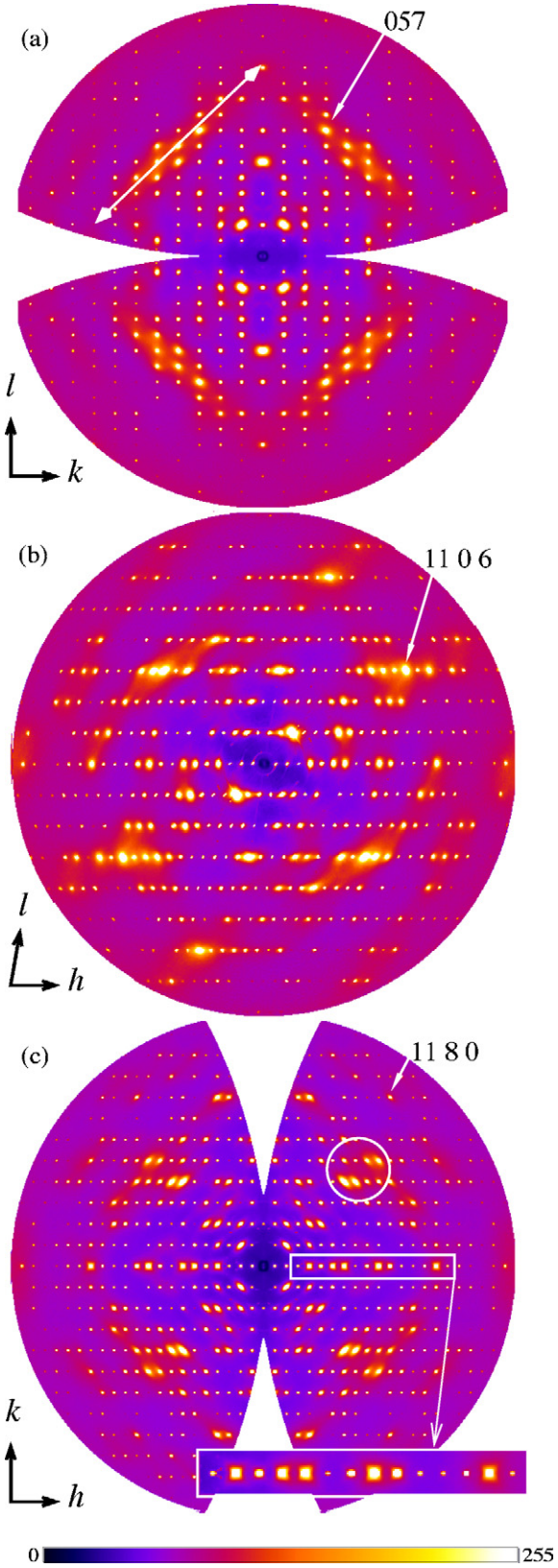

Fig. 2. The diffuse scattering in the three basal planes of Ibuprofen: (a) 0 *k l*, (b) *h* 0 *l* and (c) *h k* 0. A Bragg peak has been marked on each plane to give a sense of the extent of the data. Some key features are noted. The false colour palette is as shown, varying from black at zero scattered intensity through to white at maximum. The Bragg peaks are severely truncated on this scale.

shows the X-ray diffuse scattering in the three basal planes of Ibuprofen.

3. The modelling procedure

The data were modelled using a Monte Carlo approach (Welberry et al., 1998, 2001) in which Hooke's law springs connect the molecules and potentials are placed on selected torsional twists within the molecule (the ϕ_i angles in Fig. 1, also referred to as internal degrees of freedom, d.f.). This allows the molecules to interact, and within a molecule allows variations in molecular conformation to interact with molecular orientation and position. The result is a correlation structure in the model crystal. The model is evaluated by calculating its diffuse scattering diffraction pattern (Butler and Welberry, 1992) and comparing that with the observed scattering. When a model has been found whose diffraction pattern exhibits the key features of the observed scattering, it is refined automatically (Welberry et al., 2001).

The energy of the crystal is considered to be the sum of intra- and intermolecular contributions. The intermolecular contribution comes from the sum over the contact vectors linking the molecule with its neighbours, such that

$$E_{\text{inter}} = \sum_{\text{cv}} F_i (d_i - d_{0i})^2 \tag{1}$$

where d_i is the length of vector i connecting atoms on adjacent molecules, d_{0i} its equilibrium length and F_i is its force constant. The sum is over all contact vectors (cv).

The intramolecular energy for the model is given by summing the contributions due to the deviations from the equilibrium position over all applicable angles within each molecule, summing over any cross-terms (used to model interactions *between* the torsional d.f.), then summing over all molecules (mol). That is,

$$E_{\text{intra}} = \sum_{\text{mol}} \left(\sum_i G_i (\Delta\phi_i)^2 + \sum_{jk} G_{jk} \Delta\phi_j \Delta\phi_k \right) \tag{2}$$

where the G_i are the angular force constants for torsional angles i and $\Delta\phi_i$ are their deviations from the equilibrium value. The G_{jk} are the interaction constants for interactions between the internal torsional d.f. Evidently, for $G_{jk} > 0$, $\Delta\phi_j$ and $\Delta\phi_k$ will tend to be of opposite sign, for $G_{jk} < 0$ it will be energetically favourable for them to be of the same sign and $G_{jk} = 0$ implies they will only be correlated indirectly *via* interactions with the molecular environment.

The total energy is the sum:

$$E_{\text{total}} = E_{\text{inter}} + E_{\text{intra}} \tag{3}$$

In practice, energy is calculated for a single randomly selected molecule. The molecule's configuration is then randomly altered and its energy calculated again; the altered configuration is kept or rejected depending on the change in the energy and the temperature of the simulation.

The intermolecular contacts are a subset of all the atom–atom contacts in the system; due to limits on computation time they are *effective* interactions only. To reduce computation time further, H atoms are not used, so the contacts are C–C and O–C and O–O. Further, contacts which are likely to perform the same function in transmitting motions through the crystal are either combined into a single class, even if not symmetry equivalent, or some are simply not used. This both reduces the number of contacts over which the energy sum must be performed and, more importantly, each contact type eliminated removes a free parameter from the model.

The parameters of the model are the spring constants themselves, rather than the atomic positions as in a conventional crystallographic refinement. As the unit cells are not considered to be identical, the number of atomic positions to be found becomes very large; however, if the parameters which *determine* these positions (rather than the positions themselves) become the parameters of the model, the number of parameters to be fitted is reduced dramatically. The parameters which determine the atomic positions are the various interaction constants and the temperature, T, and are the same from unit cell to unit cell even though the instantaneous atomic positions are not.

The molecule was allowed the following degrees of freedom:

External: The position of the molecular origin, given by a 3-vector, **x**, and orientation of the molecule, given by a quaternion, a normalised 4-vector, **q**. This gives six variables to describe the molecular position and overall attitude (one component of **q** is redundant due to normalisation).

Internal: The internal coordinate system was implemented by describing the molecule using a **z**-matrix as illustrated in Table 1. Starred entries correspond to the three rotations noted in Fig. 1. All bond lengths and angles were fixed at the values given in (McConnell, 1974), but torsional rotations were allowed around three bonds: (1) The C2–C4 (effected by altering the torsional angle of atom C3, denoted ϕ_1); (2) the C2–C1 (effected by altering the torsional angle of atom O1, denoted ϕ_2); (3) C7–C10 (effected by altering the torsional angle of atom C11, denoted ϕ_3). Thus the entire molecule of fifteen non-hydrogen atoms could be described using nine variables.

These internal d.f. were chosen as, first, it was possible with them to reproduce the atomic displacement parameters deduced from a conventional single-crystal refinement and, second, further torsional degrees of freedom did not improve the model's ability to fit the observed diffuse scattering.

The intermolecular contact vectors are summarised in Table 2. Some vectors occur in pairs or triplets which, while not symmetry identical, are related—the type 16 vectors for example connect O1 to the same 'side' of the same phenyl ring, so both perform much the same function in relating the motion of the molecule to its contacting neighbour. Hence such pairs of vectors are given the same interaction constant in these simulations. Tests found that the interaction constants of contacts within the pairs could not be distinguished by the model.

4. Results and discussion

Fig. 2 shows structured diffuse scattering in the form of elongated diffuse peaks around many Bragg peaks. Overall distribution of intensity is modulated by the molecular Fourier transform; however it is also modulated by correlations in the

Table 1
A **z**-matrix containing the non-H atoms in Ibuprofen

Num.	Atom label	l	Bond length (Å)	m	Bond angle (°)	n	Dihedral angle (°)
1	C7	0	0.0000	0	0.0000	0	0.0000
2	C10	1	1.4926	0	0.0000	0	0.0000
3	C6	1	1.3917	2	120.2186	0	0.0000
4	C5	3	1.3757	1	120.7132	2	−179.0307
5	C4	4	1.3746	3	121.5883	1	−1.2481
6	C9	5	1.3806	4	118.1869	3	0.7164
7	C8	6	1.3962	5	120.7433	4	−1.2075
8	C2	5	1.5248	6	120.8730	4	178.4180
9	C3	8	1.4997	5	114.3719	6	41.1484*
10	C1	8	1.5037	9	111.7098	5	121.2775
11	O1	10	1.3056	8	115.4618	9	145.6313*
12	O2	10	1.2045	11	123.3854	8	−178.3476
13	C11	2	1.5288	1	113.9985	3	79.1683*
14	C12	13	1.5080	2	110.1695	1	−168.4420
15	C13	13	1.5184	14	111.5332	2	124.4333

Asterisk indicates those whose dihedral angle was allowed to vary. l, m and n give the connectivity of the molecule—for example C5 lies 1.3757 Å from atom 3 (C6), the C5–C6 bond makes and angle of 120.7132° to the bond between atoms 3 and 1 (C6 and C7) and the plane defined by C5, C6 and C7 makes an angle of −179.0307° to the plane defined by atoms 3, 1 and 2 (C6, C7 and C10). The atoms have been reordered relative to earlier studies (McConnell, 1974) to aid in defining the molecular flexibility, but the labels have been kept. 'Num.' is an ordinal number.

displacements of neighbouring molecules. To demonstrate this, Fig. 3 shows a calculated pattern from the $h\,k\,0$ plane assuming random displacements of a similar magnitude to those implied by the ADPs in the single-crystal studies. Plainly, some degree of correlation between the molecules is required to collapse the broad bands of intensity down into the spots seen in Fig. 2c (circled). By fitting the data in Fig. 2, it is possible to extract this correlation structure and *also* information about the 'objects' being correlated—in other words, the typical conformations of the Ibuprofen molecules.

Table 2
Summary of the contact vectors used in the simulation

Type	Origin atom	Cell translation	Symmetry (dest.)	Dest. atom	Length (Å)	M	F_i (k_BT Å^{-2})
1a	O2	0 0 0	B	O1	2.6264	2	5.6(5)
1b	O2	0 0 0	B	O2	3.2189	1	5.6(5)
1c	O1	0 0 0	B	O1	3.6342	1	5.6(5)
2a	C13	−1, −2, 0	B	C13	4.2582	1	2.3(3)
2b	C13	−1, −2, 0	B	C12	4.4752	2	2.3(3)
3a	O2	0, −1, 0	B	C9	3.2305	2	3.7(4)
3b	O2	0, −1, 0	B	C8	3.3121	2	3.7(4)
4a	C12	−1, −1, 0	B	C5	4.1044	2	3.5(5)
4b	C12	−1, −1, 0	B	C6	4.3557	2	3.5(5)
5	C11	−1, −1, 0	B	C6	4.3013	2	0.0(1)
6	C3	0, −1, 0	B	C9	4.2970	2	1.3(2)
7a	O2	0 0 0	D	C3	3.4580	2	5.2(2)
7b	O1	0 0 0	D	C3	3.9017	2	5.2(2)
8a	C12	−1, −1, 1	D	C10	4.0680	2	0.7(2)
8b	C12	−1, −1, 1	D	C6	4.2005	2	0.7(2)
9	C12	−1, 0, 1	D	C12	4.0883	2	0.9(2)
10	C12	−1, −1, 1	D	C11	4.2316	2	0.7(3)
11a	O1	0 0 1	C	C3	3.4618	2	4.6(5)
11b	O2	0 0 1	C	C3	3.7183	2	4.6(5)
12a	O1	0 0 0	C	C10	3.5534	2	3.9(1)
12b	O1	0 0 0	C	C8	3.5596	2	3.9(1)
13a	C2	0 0 0	C	C6	3.8480	2	0.4(1)
13b	C2	0 0 0	C	C8	3.8500	2	0.4(1)
14	C12	0, −1, 0	C	C6	3.9336	2	0.5(2)
15a	C13	0, −1, 0	A	C5	3.7869	2	1.3(2)
15b	C13	0, −1, 0	A	C6	3.9467	2	1.3(2)
16a	O1	0 1 0	A	C9	3.9450	2	0.8(1)
16b	O1	0 1 0	A	C8	3.8552	2	0.8(1)

One example of each is given for the molecule with the identity symmetry operator (x, y, z). Unit cell translation and symmetry of the 'destination' (dest.) (as distinct from origin) molecule of each contact is given, along with equilibrium length, multiplicity, M, and spring constant, F_i from the final simulation (uncertainty in parentheses). Symmetry operators are as follows: A $= x, y, z$, B $= -x, -y, -z$, C $= x, -(1/2) - y, -(1/2) + z$ and D $= -x, (1/2) + y, (1/2) - z$.

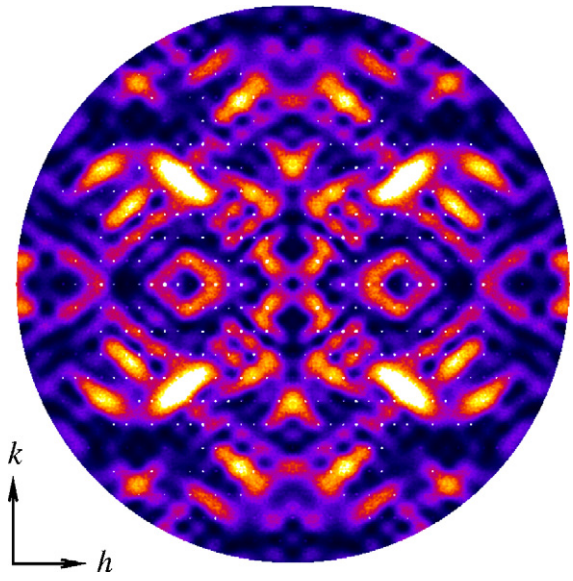

Fig. 3. Diffuse scattering in the $h\,k\,0$ plane due to random, uncorrelated displacements. Compare with Fig. 2c. The Bragg peak positions have been ANDed from the observations (white dots).

The $h\,k\,0$ plane (Fig. 2c) shows a row of cross-shaped or box-like features (indicated on the figure by a white rectangle and magnified in the inset) which suggest correlations running along directions approximately $\pm 45^\circ$ to the horizontal; this is also shown by the direction of elongation of the diffuse peaks (circled). Given that the ratio $|\mathbf{a}|/|\mathbf{b}| = 1.84 \sim 2$, this suggests interactions running along the real-space $\mathbf{a} + 2\mathbf{b}$ direction are significant. Fig. 4a shows that this direction coincides with the long axis of the molecule when projected onto the **ab** plane *and* coincides with the long direction of the pair of Ibuprofen molecules as dimerised by the –COOH–HOOC– hydrogen bonding. These features will therefore likely result from correlated motions of Ibuprofen molecules parallel to this direction.

This was tested by implementing a simple model in which the Ibuprofen molecules are linked to form chains in this $\mathbf{a} + 2\mathbf{b}$ direction. This is done by connecting the molecules using Hooke's law springs (Eq. (1)); the contact vectors resulting are shown in Fig. 4a. Other contact vectors are present in the simulation but are over an order of magnitude weaker. At this point no molecular flexibility was introduced—the molecule was treated as rigid.

It is immediately apparent from inspection of Fig. 4b that a number of key features have been produced—the diagonal oval regions of scattering, the cross or box-like shapes (highlighted by the white rectangle). The importance of these interactions agrees with the known dimerisation of the molecules joined by the H-bonds between –COOH groups (Shankland et al., 1996 for example). However, calculations of other planes of scattering ($0\,k\,l$, $h\,0\,l$) indicated that such a model was not adequate.

Inspection of the $0\,k\,l$ section (Fig. 2a) suggests that the spots are elongated along directions as indicated by the white arrow. This is not as pronounced as the effect seen in $h\,k\,0$ and so

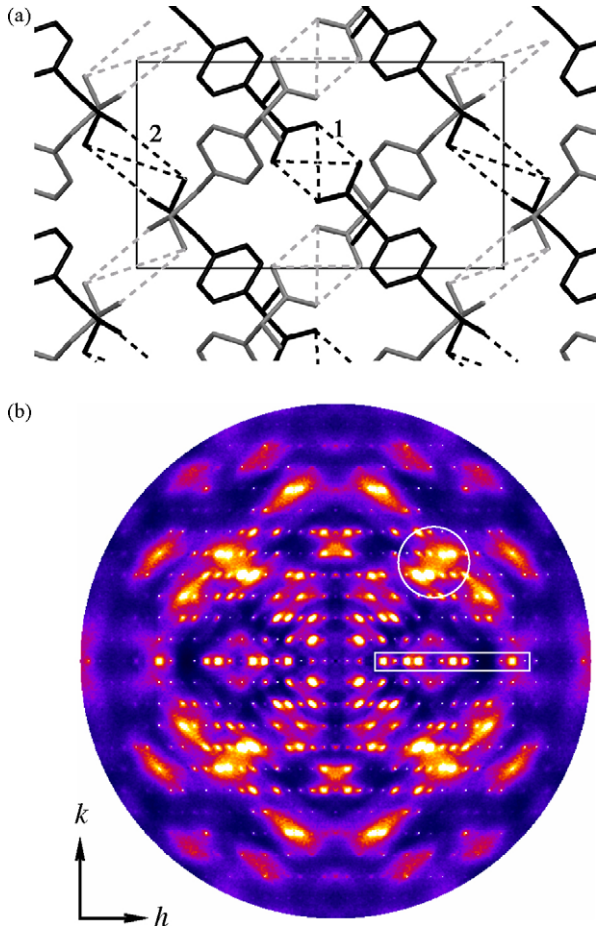

Fig. 4. (a) A section of the model crystal showing as dashed lines the interactions that combine to give chains of molecules running diagonally through the **ab** ($h\ h$) plane. The unit cell is shown with **a** horizontal and **b** vertical. '1' indicates contact vectors of types 1a, b & c (–COOH–HOOC–); '2' indicates vectors of types 2a & b. Grey molecules and contacts form chains along $\mathbf{a} + 2\mathbf{b}$, black molecules and contact vectors form chains along $\mathbf{a} - 2\mathbf{b}$. (b) The diffuse scattering in the $h\,k\,0$ plane from a model in which the **ab** plane interactions shown in (a) dominate. Compare with Figs. 2c and 3. The Bragg peak positions have been ANDed from the observations (white dots).

this suggests that correlations exist in that plane, but are relatively weak. The $h\,0\,l$ plane (Fig. 2b) shows little collapsing of the thermal diffuse scattering into structured shapes. The peaks are generally narrower along a direction pointing radially out from the centre, but the lack of azimuthal variation of the effect suggests weak, relatively isotropic interactions.

These considerations suggest that a model needs strong interactions along the diagonals through the **ab** plane, weaker along the diagonals through the **bc** plane and weak, isotropic interactions in the **ac** plane.

Such a model was implemented. Molecular flexibility was introduced with associated cross-terms between torsion angles. Initially, the torsional angles on C3, O1, C11 and C12 were allowed to vary. Qualitative tests of the model against the observed data showed that the torsional angle on C12 could be fixed at its average value, with the result that the final model used three torsional angles plus a single cross-term between the torsional angles on C3 and O1 (that is, between ϕ_1 and ϕ_2).

The model was iteratively refined following the procedure put forward previously (Welberry et al., 1998, 2001). Final calculated diffuse scattering patterns are shown in Fig. 5. The agreement with those shown in Fig. 2 is good, with all the major features captured. The relative magnitudes of features are correct, indicating that the model shows the correct size for the thermal motions.

The spring constants and contact vector groupings of the final model are summarised in Table 2. Vectors which were 'grouped' in the refinement – given the same spring constant – are indicated by the numbering scheme, for example 3a and 3b are symmetrically inequivalent vectors which were grouped together insofar as they were given the same interaction constant. The spring constants on the torsion angles were refined to be:

- $G_1 = 1.4(2) \times 10^2\, k_B T$ degree^{-2} (atom C3).
- $G_2 = 1.2(2) \times 10^2\, k_B T$ degree^{-2} (O1).
- $G_3 = 3.4(2) \times 10^2\, k_B T$ degree^{-2} (C11).
- $G_{1,2} = 2.4(1) \times 10^2\, k_B T$ degree^{-2} (cross-term between ϕ_1 (C3) and ϕ_2 (O1)).

Type 1 contact vectors are responsible for dimerisation of the pairs of Ibuprofen molecules, and it is not surprising that this proves to be the biggest interaction. Beyond that, it must be recalled that the contact vectors are a mechanism to produce a correlation structure which gives the observed diffuse scattering. They operate in a highly cooperative fashion, and interpretation of individual spring constants is not expected to be meaningful. The correlation structure is the key result of the simulation process, the interaction potentials are not, they are a means of inducing it.

The final R factor, as calculated in earlier work (Welberry et al., 2001), was found to be 26.7%, which seems large but it must be recalled that this is calculated from approximately 1.2×10^5 data points, many of which contain little signal. Further, the study focusses on the weak features—the Bragg peaks, which contain high signal-to-noise, are explicitly excised from the calculation.

The assumption is that a model which gives a good fit to the observed data contains molecular conformations and intermolecular correlations which are representative of those found in the real crystal. Hence, the model can be mined for insight into the real system. In particular, the goal is to map out aspects of the conformational space of the molecule in the crystal and the short-range correlation structure.

A key point is that this work does not look at averages across crystal structures but the molecular conformations that go into that average. This is different from, for example, database mining which essentially looks at trends in the behaviour of average structures determined from single-crystal Bragg diffraction.

The displacements of the atoms in a given molecule away from their average positions can be determined, and itself averaged. This can be compared with the same result for the molecule's neighbours; further, the component of this average displacement in a given direction can be found, and correlations between these components calculated across the model crystal. This gives rise to a plot of correlation coefficient against dis-

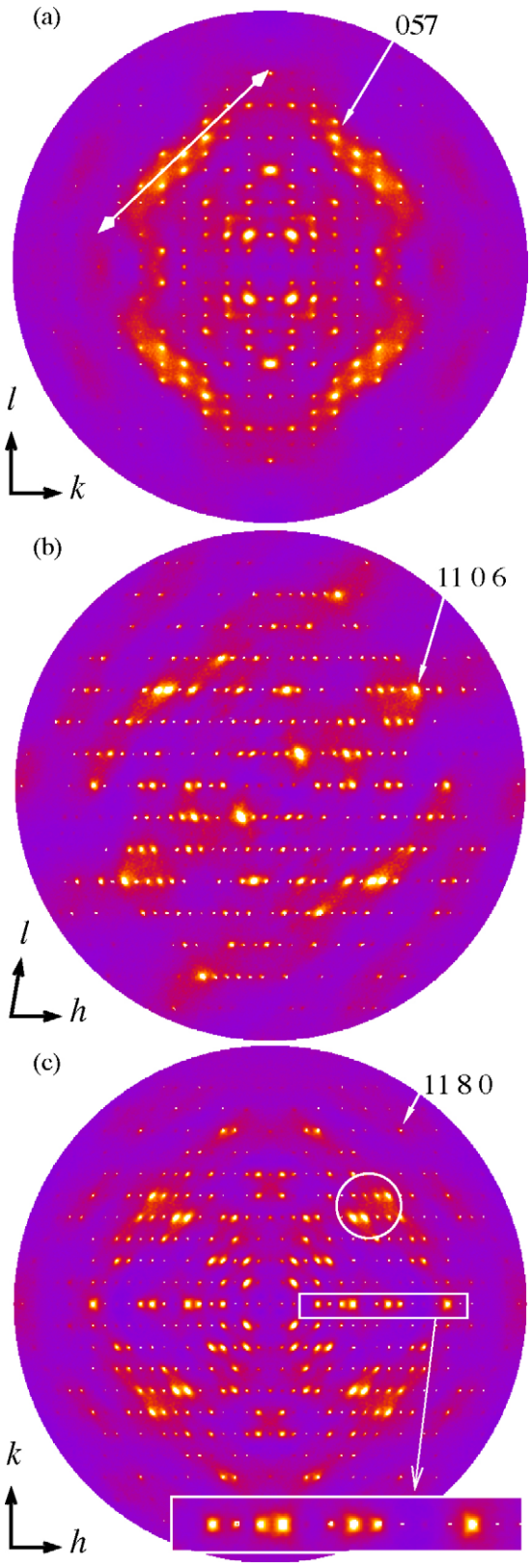

Fig. 5. The diffuse scattering in the three basal planes of Ibuprofen, calculated from the final model: (a) $0\,k\,l$, (b) $h\,0\,l$ and (c) $h\,k\,0$. Bragg peaks from the observations have been ANDed to make the images more comparable with those in Fig. 2.

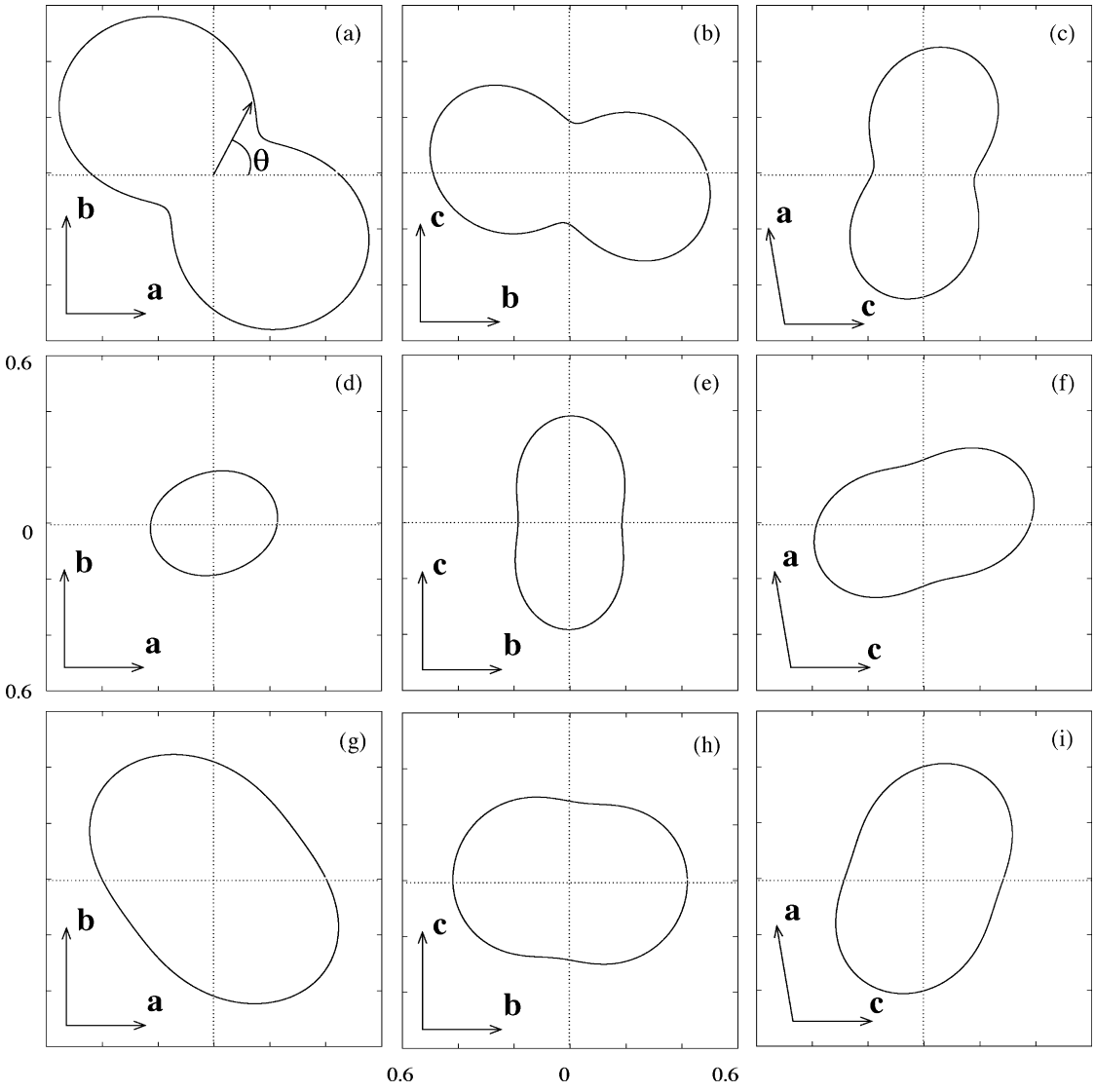

Fig. 6. Correlations between molecules connected by contact vectors of type 1 (top row), type 2 (middle row) & type 3 (bottom row) in the three basal planes of Ibuprofen. The length of the radial vector gives the correlation between the components of the displacements at an angle of θ to the horizontal axis for molecules connected by the contact vector in question. Note that in the **ab** and **bc** planes equivalent figures, but mirrored, can be generated if a different molecule in the unit cell is chosen as the origin for the calculation.

placement direction. This can be done for each contact vector, which by implication means for each type of nearest-neighbour molecular pair in the crystal. Fig. 6a shows that for molecules connected by the dimerising vectors (types 1a, b & c), displacements of the molecules away from the average position in the direction of the vector connecting the centres of the two contacting molecules ($\pm 45^\circ$ to the **a** direction) are strongly correlated, while those perpendicular to this (at least within the **ab** plane) are weakly correlated. In other words, the correlations in the molecular motions are longitudinal along the vector direction, hardly a surprising result. Fig. 6b and c shows that the neighbours connected by this contact are strongly correlated in all three basal planes. In all cases, the direction of maximum correlation is approximately the direction from the centre of mass of one molecule to that of the contacting neighbour as projected onto the plane of interest, and the correlations in directions perpendicular are weak.

Fig. 6d–f shows the same results for the vectors of type 2 (2a and 2b). For such neighbours, there is little apparent correlation amongst the displacements that lie in the **ab** plane, but both Fig. 6e and f shows significant correlation in the **c** component of the molecular displacements.

Despite connecting different pairs of molecules, contact vector type 3 (Fig. 6g–i) nevertheless show a very similar pattern of correlations in the displacements to type 1. In this case, the neighbours are at 90° to the chains shown in Fig. 4a. This, combined with the results for contact vector type 1, shows that the molecules in the **ab** plane are, on the scale of this fairly flexible system, quite strongly interacting even apart from the dimerising interaction. If the interactions in the **ab** plane were purely along the chains, the correlation would be one-dimensional and the scattering would collapse into planes, whereas clearly it collapses into spots, albeit elongated spots. Agreeing with this are other large correlations in the **ab** plane induced by the many

contact vectors that propagate along the **b** axis, such as types 15 & 16. For these contact vectors the **b** direction components of the displacements are most strongly correlated (correlation coefficient of ~ 0.45).

The conclusion that the intermolecular contacts are significant enough to induce substantial intermolecular displacive correlations leads to an exploration of the conformational energy of the molecule *within* the crystal lattice. Calculation of molecular energies as a function of their torsional degrees of freedom can be performed to a high degree of precision for isolated molecules. However, crystal structure is a result of the interactions between molecules as well as the possible conformations the molecules themselves can take. For example it is possible to examine the conformation space of a molecule within the crystalline environment. This must be done with the caveat that the potentials used to model the intra- and intermolecular interactions are simple approximations of the real ones. In particular, the parabolic potential on the lengths of the contact vectors is not expected to work for large variations in their lengths, particularly when the vectors are shortened—plainly an interatomic distance can increase indefinitely whereas it cannot decrease beyond limits set by coulomb repulsion. However, implementing such considerations adds extra parameters to the model (if, for example, the potentials become functions of more than one variable), slowing down already lengthy calculations and increasing the dimensionality of the parameter space being searched. Hence there must be a strong, demonstrated need for these developments—a need which can only be demonstrated by exploring the current model.

Fig. 7 shows a scatter plot of the distribution of ϕ_1, the torsional angle on C3, and ϕ_2, the torsion angle on O1, that minimises the molecular energies, calculated for each molecule in the final simulation. The plot shows that there is a relationship between the angles, with the crystal able to accommodate a wider range of values for ϕ_1 (rotations around the C2–C4 bond). Fig. 2 of (Shankland et al., 1998) shows a scatter plot of the occurrence of torsional angle around the C1–C2 bond (analogous to ϕ_2) against the torsional angle around the C2–C4 bond (analogous to ϕ_1) as determined from a range of average structures of molecules which contain Ibuprofen-like fragments. The plot shows the same conclusion as Fig. 7 in that the distribution is much narrower in terms of torsional angles around the C1–C2 bond than around the C2–C4 bond.

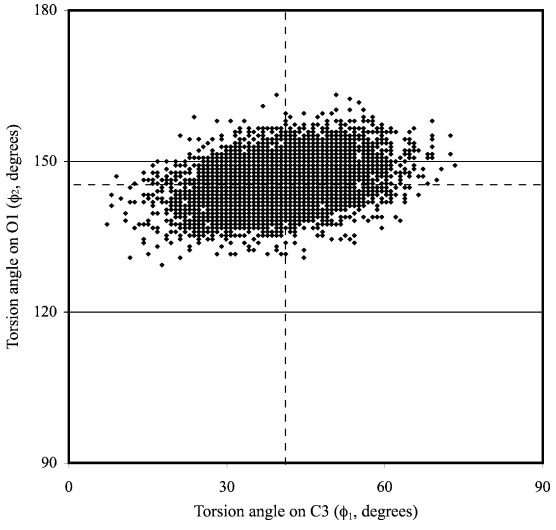

Fig. 7. A scatter plot of the distribution of the values of the dihedral angles on C3 (ϕ_1) and O1 (ϕ_2) that give minimum molecular energy. Dashed lines show the equilibrium values (see Table 1).

Fig. 7 shows a small positive slope (correlation coefficient is 0.36), as would be expected given the sign of the cross-term between these torsional twists. Due to atom ordering in the definitions of the angles in the z-matrix, this implies that they move in counter-motion.

A simple way to look at molecular conformation is to calculate correlations between the variables used to describe a molecule. Table 3 shows these correlations. Plainly components of the quaternion which orients the molecule are correlated through normalisation of that 4-vector. Another large correlation is that between ϕ_1 and ϕ_3. Weak correlations exists between the positional variables, x, y and z, and the others. Strong correlations exist between the quaternion components (q_i) and the torsional angles (ϕ_i). This is because the torsional angles act to reorient large subsections of the molecule, something which can be compensated for by reorienting the molecule as a whole.

The large negative correlations between ϕ_1 and ϕ_3 (torsional angles on C3 and C11) is a result of the molecule as a whole minimising its energy subject to the contacts with the surrounding molecules; there is no direct interaction between these variables in the energy expression. This suggests that care must be taken when using molecular fragments found in related systems as a guide to what conformations might be expected in a particular system. Degrees of freedom in what might seem to be an unrelated fragment may have a strong effect on the fragment in question.

It is apparent that the correlation between motions around ϕ_1 and ϕ_2 is quite weak—weaker than the correlation suggested by Fig. 7. This is because the crystal is at thermal equilibrium and many molecules are not in their lowest energy 'states.

Extending this, correlations between variables on adjacent molecules can be examined. Some examples are given in Table 4, which shows that for molecules connected by contact vectors of type 1, the molecular origin x and y coordinates are substantially correlated, but the torsional twists are not propagated. For molecules connected by contact vectors of type 2, the molecular origin y and z coordinates are substantially correlated, and again the torsional twists are not propagated. For molecules connected by contact vectors of type 3, all three components of the molecular origin coordinate are substantially correlated, and again the torsional twists are not propagated. Further, in all cases the torsional twists are seen to be independent of the displacement on the neighbouring molecule. Hence it is really only motions parallel with the contact vector direction which are transmitted, and shearing motions, whether they seek to cause rotations or lateral motions in the neighbouring molecule, are not important in generating a model of the crys-

Table 3
Correlations between the variables used to describe a molecule

	x	y	z	q_1	q_2	q_3	q_4	ϕ_1	ϕ_2	ϕ_3
x	1.0									
y	−0.06	1.0								
z	−0.05	−0.04	1.0							
q_1	0.09	−0.06	0.08	1.0						
q_2	0.29	−0.21	0.08	0.79	1.0					
q_3	−0.28	0.22	0.32	−0.57	−0.66	1.0				
q_4	−0.11	0.09	0.12	−0.90	−0.67	0.74	1.0			
ϕ_1	−0.18	0.15	−0.09	−0.89	−0.62	0.49	0.83	1.0		
ϕ_2	−0.12	0.09	0.01	−0.21	− 0.34	0.34	0.23	0.11	1.0	
ϕ_3	−0.20	0.14	−0.01	0.60	0.31	−0.23	−0.56	−0.51	−0.05	1.0

x, y and z are the Cartesian coordinates of the origin atom (atom C7), the q_i are the components of the quaternion that give the orientation of the first bond in the molecule (C7 to C10) while the ϕ_i are the allowed torsional rotations. Note that correlations amongst the q_i are not meaningful as the quaternion is normalised.

Table 4
Correlations between the variables on adjacent molecules (A and B)

	x_A	y_A	z_A	ϕ_{A1}	ϕ_{A2}	ϕ_{A3}
Type 1						
x_B	0.32					
y_B	−0.16	0.26				
z_B	−0.05	0.03	0.12			
ϕ_{B1}	0.00	0.02	0.01	0.02		
ϕ_{B2}	−0.06	0.03	0.00	0.01	0.06	
ϕ_{B3}	−0.03	0.023	−0.01	−0.03	−0.01	0.00
Type 2						
x_B	0.13					
y_B	−0.05	0.29				
z_B	0.03	−0.18	0.35			
ϕ_{B1}	0.03	−0.03	0.04	0.03		
ϕ_{B2}	0.05	−0.07	0.05	0.02	−0.02	
ϕ_{B3}	0.07	−0.08	0.08	−0.01	−0.03	−0.02
Type 3						
x_B	0.24					
y_B	0.01	0.25				
z_B	0.03	−0.01	0.21			
ϕ_{B1}	0.02	−0.02	0.04	0.06		
ϕ_{B2}	0.05	−0.01	−0.01	0.01	−0.03	
ϕ_{B3}	−0.05	0.00	0.00	0.01	0.01	−0.02

x, y and z are the Cartesian coordinates of the origin atom (atom C7) and the ϕ_i are the allowed torsional rotations. Correlations are between molecules connected by the given contact vector types.

tal which does a good job of reproducing the observed diffuse scattering.

5. Conclusions

It has been shown that the diffuse scattering from a molecular crystal can be modelled using a Monte Carlo modelling approach. The resulting model crystal can then be mined for information. The model gives information on the population of molecular conformations, and shows how the conformation and overall orientation of one molecule correlates with the conformations and overall orientations of its neighbours. Atomic displacement parameters determined from conventional single-crystal studies are valuable in finding the degrees of flexibility a molecule requires (in this case, torsional rotations around three bonds).

For Ibuprofen, the strongest contact vector was found to coincide with the –COOH–HOOC– interaction which dimerises pairs of molecules. Important molecular degrees of freedom were torsional motions of C3 (angle ϕ_1), O1 (angle ϕ_2) and C11 (angle ϕ_3). Of these, the motions of C1 and O1 interact directly but weakly *via* a cross-term in the energy, while C3 and C11 are substantially negatively correlated indirectly by the network of contact vectors.

Between molecules, components of the positional coordinates are correlated when they coincide with the direction of propagation of important intermolecular contacts, but motions perpendicular to such contacts, and rotation about the torsional angles, do not propagate strongly from molecule to molecule.

Acknowledgements

The authors would like to thank the Australia Research Council and the Australian Synchrotron Research Program for financial support and the Australian Partnership for Advanced Computing for computer time. We are grateful to Dr. Tony Willis of RSC for single-crystal Bragg data collection and to Dr. Peter Lee of the Advanced Photon Source for help with diffuse scattering data collection.

References

Butler, B.D., Welberry, T.R., 1992. J. Appl. Cryst. 25, 391–399.
Cano, H., Gabas, N., Canselier, J.P., 2001. J. Cryst. Growth 224, 335.
Estermann, M.A., Steurer, W., 1998. Phase Transit. 67, 165.
Labhasetwar, V., Deshmukh, S.V., Dorle, A.K., 1993. Drug Dev. Ind. Pharm. 19, 631.
McConnell, J.F., 1974. Cryst. Struct. Commun. 3, 73.
Perlovich, G.L., Kurkov, S.V., Hansen, L.K., Bauer-Brandl, A., 2004. J. Pharm. Sci. 93, 654.
Scheidegger, S., Estermann, M.A., Steurer, W., 2000. J. Appl. Cryst. 33, 35.
Shankland, N., Florence, A.J., Cox, P.J., Sheen, D.B., Love, S.W., Stewart, N.S., Wilson, C.C., 1996. Chem. Commun., 855.
Shankland, N., Wilson, C.C., Florence, A.J., Cox, P.J., 1997. Acta Crystallogr. C 53, 951.

Shankland, N., Florence, A.J., Cox, P.J., Wilson, C.C., Shankland, K., 1998. Int. J. Pharm. 165, 107.
Weber, T., Estermann, M.A., Bürgi, H.-B., 2001. Acta Crystallogr. B 57, 579.
Welberry, T.R., 2004. Diffuse X-ray Scattering and Models of Disorder, OUP.
Welberry, T.R., Proffen, T., Bown, M., 1998. Acta Crystallogr. A 54, 661–674.
Welberry, T.R., Goossens, D.J., Edwards, A.J., David, W.I.F., 2001. Acta Crystallogr. A 57, 101–109.
Welberry, T.R., Goossens, D.J., Heerdegen, A.P., Lee, P.L., 2005. Z. Krist. 220, 1052.
Winn, D., Doherty, M.F., 1998. AIChE J. 44, 2501.